LETTERS

An anomalous positron abundance in cosmic rays with energies 1.5–100 GeV

O. Adriani[1,2], G. C. Barbarino[3,4], G. A. Bazilevskaya[5], R. Bellotti[6,7], M. Boezio[8], E. A. Bogomolov[9], L. Bonechi[1,2], M. Bongi[2], V. Bonvicini[8], S. Bottai[2], A. Bruno[6,7], F. Cafagna[7], D. Campana[4], P. Carlson[10], M. Casolino[11], G. Castellini[12], M. P. De Pascale[11,13], G. De Rosa[4], N. De Simone[11,13], V. Di Felice[11,13], A. M. Galper[14], L. Grishantseva[14], P. Hofverberg[10], S. V. Koldashov[14], S. Y. Krutkov[9], A. N. Kvashnin[5], A. Leonov[14], V. Malvezzi[11], L. Marcelli[11], W. Menn[15], V. V. Mikhailov[14], E. Mocchiutti[8], S. Orsi[10,11], G. Osteria[4], P. Papini[2], M. Pearce[16], P. Picozza[11,13], M. Ricci[17], S. B. Ricciarini[2], M. Simon[15], R. Sparvoli[11,13], P. Spillantini[1,2], Y. I. Stozhkov[5], A. Vacchi[8], E. Vannuccini[2], G. Vasilyev[9], S. A. Voronov[14], Y. T. Yurkin[14], G. Zampa[8], N. Zampa[8] & V. G. Zverev[14]

Antiparticles account for a small fraction of cosmic rays and are known to be produced in interactions between cosmic-ray nuclei and atoms in the interstellar medium[1], which is referred to as a 'secondary source'. Positrons might also originate in objects such as pulsars[2] and microquasars[3] or through dark matter annihilation[4], which would be 'primary sources'. Previous statistically limited measurements[5–7] of the ratio of positron and electron fluxes have been interpreted as evidence for a primary source for the positrons, as has an increase in the total electron+positron flux at energies between 300 and 600 GeV (ref. 8). Here we report a measurement of the positron fraction in the energy range 1.5–100 GeV. We find that the positron fraction increases sharply over much of that range, in a way that appears to be completely inconsistent with secondary sources. We therefore conclude that a primary source, be it an astrophysical object or dark matter annihilation, is necessary.

The results presented here are based on the data set collected by the PAMELA satellite-borne experiment[9] between July 2006 and February 2008. More than 10^9 triggers were accumulated during a total acquisition time of approximately 500 days. From these triggered events, 151,672 electrons and 9,430 positrons were identified in the energy interval 1.5–100 GeV. Results are presented as positron fraction—that is, the ratio of positron flux to the sum of electron and positron fluxes, $\phi(e^+)/(\phi(e^+)+\phi(e^-))$—and are shown in Table 1. The apparatus is a system of electronic particle detectors optimized for the study of antiparticles in the cosmic radiation (Supplementary Information section 1). It was launched from the Bajkonur cosmodrome on 15 June 2006 on board a satellite that was placed into a 70.0° inclination orbit, at an altitude varying between 350 km and 610 km. A permanent magnet spectrometer with a silicon tracking system allows the rigidity (momentum/charge, resulting in units of GV), and sign-of-charge of the incident particle to be determined. The interaction pattern in an imaging silicon-tungsten calorimeter allows electrons and positrons to be separated from protons.

The misidentification of protons is the largest source of background when estimating the positron fraction. This can occur if electron- and proton-like interaction patterns are confused in the calorimeter data. The proton-to-positron flux ratio increases from approximately 10^3 at 1 GV to approximately 10^4 at 100 GV. Robust positron identification is therefore required, and the residual proton background must be estimated accurately. The imaging calorimeter is 16.3 radiation lengths (0.6 nuclear interaction lengths) deep, so electrons and positrons develop well contained electromagnetic showers in the energy range of interest. In contrast, the majority of the protons will either pass through the calorimeter as minimum ionizing particles or interact deep in the calorimeter.

This is illustrated in Fig. 1, which shows $\mathcal{F}$, the fraction of calorimeter energy deposited inside a cylinder of radius 0.3 Molière radii, as a function of deflection (rigidity^{-1}). The axis of the cylinder is defined by extrapolating the particle track reconstructed in the spectrometer. For negatively-signed deflections, electrons are clearly visible as a horizontal band with $\mathcal{F}$ lying mostly between 0.4 and 0.7. For positively-signed deflections, the similar horizontal band is naturally associated with positrons, with the remaining points, mostly at $\mathcal{F} < 0.4$, designated as proton contamination (see Supplementary Information sections 2 and 3 for additional details concerning particle selection and background determination).

Figure 2 shows the positron fraction measured by the PAMELA experiment compared with other recent experimental data. The PAMELA data covers the energy range 1.5–100 GeV, with significantly higher statistics than other measurements. Two features are clearly visible in the data. At low energies (below 5 GeV) the PAMELA results are systematically lower than data collected during the 1990s, and at high energies (above 10 GeV) the PAMELA results show that the positron fraction increases significantly with energy.

Measurements of cosmic-ray positrons and electrons address a number of questions in contemporary astrophysics, such as the nature and distribution of particle sources in our Galaxy, and the subsequent propagation of cosmic rays through the Galaxy and the solar heliosphere. Positrons are believed to be mainly created in secondary production processes, that is, by the interaction of cosmic-ray nuclei with the interstellar gas. The solid line in Fig. 2 shows a calculation[1] based on such an assumption. Although this calculation is widely used, it does

[1]University of Florence, Department of Physics, Via Sansone 1, I-50019 Sesto Fiorentino, Florence, Italy. [2]INFN, Sezione di Florence, Via Sansone 1, I-50019 Sesto Fiorentino, Florence, Italy. [3]University of Naples "Federico II", Department of Physics, Via Cintia, I-80126 Naples, Italy. [4]INFN, Sezione di Naples, Via Cintia, I-80126 Naples, Italy. [5]Lebedev Physical Institute, Leninsky Prospekt 53, RU-119991 Moscow, Russia. [6]University of Bari, Department of Physics, Via Amendola 173, I-70126 Bari, Italy. [7]INFN, Sezione di Bari, Via Amendola 173, I-70126 Bari, Italy. [8]INFN, Sezione di Trieste, Padriciano 99, I-34012 Trieste, Italy. [9]Ioffe Physical Technical Institute, Polytekhnicheskaya 26, RU-194021 St Petersburg, Russia. [10]KTH, Department of Physics, AlbaNova University Centre, SE-10691 Stockholm, Sweden. [11]INFN, Sezione di Roma "Tor Vergata", Via della Ricerca Scientifica 1, I-00133 Rome, Italy. [12]IFAC, Via Madonna del Piano 10, I-50019 Sesto Fiorentino, Florence, Italy. [13]University of Rome "Tor Vergata", Department of Physics, Via della Ricerca Scientifica 1, I-00133 Rome, Italy. [14]Moscow Engineering and Physics Institute, Kashirskoe Shosse 31, RU-11540 Moscow, Russia. [15]Universität Siegen, D-57068 Siegen, Germany. [16]KTH, Department of Physics and The Oskar Klein Centre for Cosmoparticle Physics, AlbaNova University Centre, SE-10691 Stockholm, Sweden. [17]INFN, Laboratori Nazionali di Frascati, Via Enrico Fermi 40, I-00044 Frascati, Italy.

Table 1 | Summary of positron fraction results

Rigidity at spectrometer (GV)	Mean kinetic energy at top of payload (GeV)	Extrapolated $\frac{\phi(e^+)}{(\phi(e^+)+\phi(e^-))}$ at top of payload
1.5–1.8	1.64	$(0.0673^{+0.0014}_{-0.0013})$
1.8–2.2	1.99	(0.0607 ± 0.0012)
2.2–2.7	2.44	(0.0583 ± 0.0011)
2.7–3.3	2.99	(0.0551 ± 0.0012)
3.3–4.1	3.68	(0.0550 ± 0.0012)
4.1–5.0	4.52	(0.0502 ± 0.0014)
5.0–6.1	5.43	(0.0548 ± 0.0016)
6.1–7.4	6.83	(0.0483 ± 0.0018)
7.4–9.1	8.28	(0.0529 ± 0.0023)
9.1–11.2	10.17	$(0.0546^{+0.0029}_{-0.0028})$
11.2–15.0	13.11	$(0.0585^{+0.0030}_{-0.0031})$
15.0–20.0	17.52	$(0.0590^{+0.0040}_{-0.0041})$
20.0–28.0	24.02	(0.0746 ± 0.0059)
28.0–42.0	35.01	(0.0831 ± 0.0093)
42.0–65.0	53.52	$(0.106^{+0.022}_{-0.023})$
65.0–100.0	82.55	$(0.137^{+0.048}_{-0.043})$

The errors are one standard deviation. Details concerning particle selection and proton background determination can be found in Supplementary Information sections 2 and 3. The detection efficiencies for electrons and positrons are assumed to cancel, as the physical processes that these species undergo in the PAMELA detectors can be assumed to be identical across the energy range of interest. Possible bias arising from a sign-of-charge dependence on the acceptance due to the spectrometer magnetic field configuration and east–west effects caused by the Earth's magnetic field were excluded as follows. Effects due to the spectrometer magnetic field were studied using the PAMELA Collaboration's simulation software. No significant difference was found between the electron and positron detection efficiency above 1 GV. East–west effects, as well as contamination from re-entrant albedo particles (secondary particles produced by cosmic rays interacting with the Earth's atmosphere that are scattered upward but lack sufficient energy to leave the Earth's magnetic field and re-enter the atmosphere in the opposite hemisphere but at a similar magnetic latitude), are significant around and below the lowest permitted rigidity for a charged cosmic ray to reach the Earth from infinite distance, known as the geomagnetic cut-off. The geomagnetic cut-off for the PAMELA orbit varies from less than 100 MV for the highest orbital latitudes to ~15 GV for equatorial regions. In this work, only events with a measured rigidity exceeding the estimated vertical (PAMELA z-axis) geomagnetic cut-off by a factor of 1.3 were considered. This reduced east–west effects and re-entrant particle contamination to a negligible amount. The vertical geomagnetic cut-off was determined following the Størmer formalism on an event-by-event basis and using orbital parameters reconstructed at a rate of 1 Hz.

not account for uncertainties related to the production of secondary positrons and electrons (see ref. 10). Uncertainties arise because of incomplete knowledge of (1) the primary cosmic-ray nuclei spectra, (2) modelling of interaction cross-sections, (3) modelling of cosmic-ray propagation in the Galaxy and (4) solar modulation effects.

The low energy data from previous experiments (CAPRICE94[11], HEAT95[6] and AMS-01[12]) match the calculated secondary fraction while the PAMELA data are clearly lower. This points to charge-sign-dependent solar modulation effects. The solar wind modifies the energy spectra of cosmic rays within the Solar System. This effect is called solar modulation, and has a significant effect on cosmic rays with energies less than about 10 GeV. The amount of solar modulation depends on solar activity, which has an approximately sinusoidal time dependence and is most evident at solar maximum, when the low-energy cosmic-ray flux is at a minimum. The peak-to-peak period is 11 years, but a complete 'solar cycle' is 22 years long because at each maximum the polarity of the solar magnetic field reverses. The low energy difference between the PAMELA and other, older, results can be interpreted as a consequence of charge dependent solar modulation effects (Supplementary Information section 4). These older results were collected during the previous polarity of the solar cycle. A balloon-borne experiment which flew in June 2006 has also observed a suppressed positron fraction[13] at low energies, but with large statistical uncertainties.

Above 5 GeV, the PAMELA positron fraction agrees with the most recent measurements[5–7]. Although too statistically limited to draw any significant conclusions, these high energy measurements indicate a flatter positron fraction than expected from secondary production models. Now, PAMELA data clearly show that the positron fraction increases significantly with energy. Besides the uncertainties previously discussed, those on the primary electron spectrum are also relevant. The electron injection spectrum at source is expected to have a power law index of approximately −2 (ref. 14) and be equal to that of protons[15] up to about 1 TeV. When the energy losses of

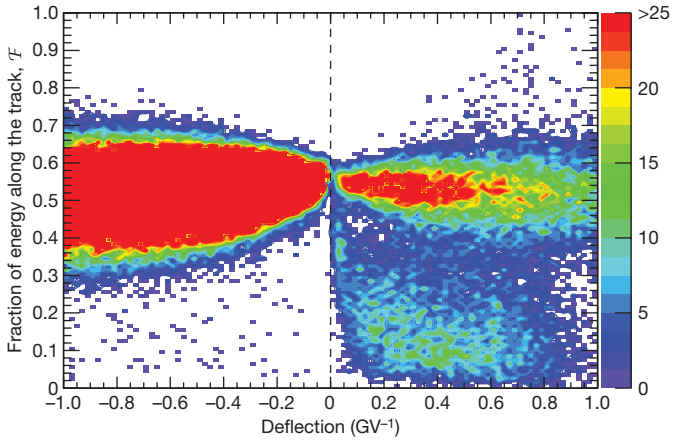

Figure 1 | Calorimeter energy fraction, $\mathcal{F}$. The fraction of calorimeter energy deposited inside a cylinder of radius 0.3 Molière radii, as a function of deflection. The number of events per bin is shown in different colours, as indicated in the colour scale. The axis of the cylinder is defined by extrapolating the particle track reconstructed by the spectrometer. The Molière radius is an important quantity in calorimetry, as it quantifies the lateral spread of an electromagnetic shower (about 90% of the shower energy is contained in a cylinder with a radius equal to 1 Molière radius), and depends only on the absorbing material (tungsten in this case). The events were selected requiring a match between the momentum measured by the tracking system and the total detected energy and requiring that the electromagnetic shower starts developing in the first planes of the calorimeter. The particle identification was tuned to reject 99.9% of the protons, while selecting >95% of the electrons or positrons.

primary cosmic rays during their propagation are taken into account, electrons are expected to have a harder spectrum than positrons if these are mostly of secondary origin. Hence, the positron fraction is expected to fall as a smooth function of increasing energy. Therefore, PAMELA positron fraction data cannot be understood by standard models describing the secondary production of cosmic rays. Either a significant modification in the acceleration and propagation models for cosmic rays is needed, or a primary component is present (for more details, see ref. 16). There are several interesting candidates for a primary component, including the annihilation of dark matter particles in the vicinity of our Galaxy and a contribution from nearby astrophysical sources, such as pulsars or microquasars.

The energy budget of the Universe can be broken down into baryonic matter (about 5%), dark matter (about 23%) and dark energy (about 72%)[17]. Many particle candidates have been proposed for the dark matter component. The most widely studied are weakly interacting massive particles (WIMPs), such as the neutralino from supersymmetric models[4] and the lightest Kaluza Klein particle from extra dimension models[18,19]. High energy antiparticles such as positrons and antiprotons (see ref. 20 and references within) can be produced during the annihilation or decay of these dark matter particles in our Galaxy. In a previous publication[21], we presented the antiproton-to-proton flux ratio in the energy range 1–100 GeV. The data follow the trend expected from secondary production calculations for antiprotons. Therefore, if the PAMELA positron results have a component due to dark matter this has to annihilate or decay into mostly leptonic final states. Furthermore, heavy WIMP candidates or large boost factors (see, for example, refs 22, 23) associated with non-uniform clumps in the dark matter distribution are required. It is worth pointing out that our antiproton-to-proton flux ratio data[21] limit significantly the boost factor for thermal WIMP candidates (ref. 24). WIMPs of non-thermal origin[25] can also be considered as explanations for both PAMELA positron and antiproton results. This model predicts a sharp decrease in the primary positron spectrum above 100 GeV, an energy range that PAMELA is exploring and will be soon able to clarify.

The possible production of positrons from nearby astrophysical sources, such as pulsars[2,26,27] and microquasars[3], must be taken into

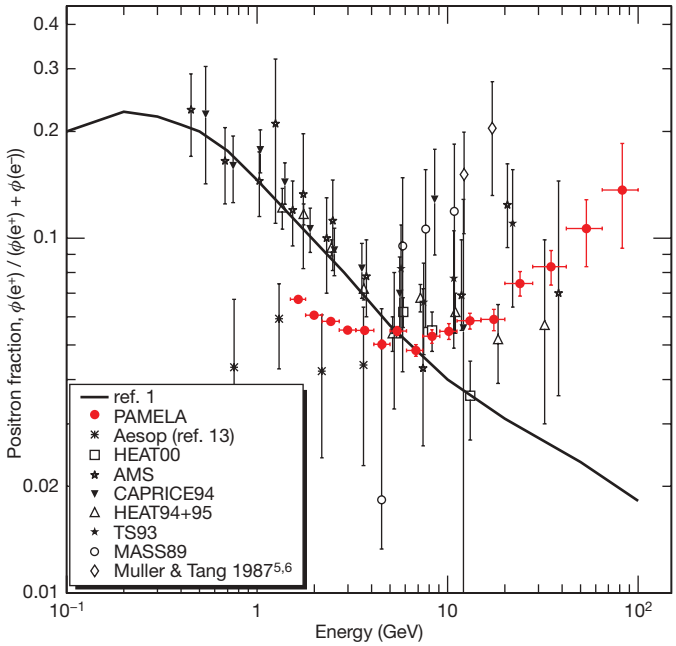

Figure 2 | PAMELA positron fraction with other experimental data and with secondary production model. The positron fraction measured by the PAMELA experiment compared with other recent experimental data (see refs 5–7, 11–13, 30, and references within). The solid line shows a calculation[1] for pure secondary production of positrons during the propagation of cosmic rays in the Galaxy without reacceleration processes. Error bars show 1 s.d.; if not visible, they lie inside the data points.

account when interpreting potential dark matter signals. A pulsar magnetosphere is a well known cosmic particle accelerator. The details of the acceleration processes are as yet unclear, but electrons are expected to be accelerated in the magnetosphere, where they induce an electromagnetic cascade. This process results in electrons and positrons that can escape into the interstellar medium, contributing to the cosmic-ray electron and positron components. As the energy spectrum of these particles is expected to be harder than that of the secondary positrons, such pulsar-originated positrons may dominate the high energy end of the cosmic-ray positron spectrum. But because of the energy losses of electrons and positrons during their propagation, just one or a few nearby pulsars can contribute significantly to the positron energy spectrum (see, for example, refs 28, 29).

The PAMELA positron data presented here are insufficient to distinguish between astrophysical primary sources and dark matter annihilation. However, PAMELA will soon present results concerning the energy spectra of primary cosmic rays—such as electrons, protons and higher mass nuclei—that will significantly constrain the secondary production models, thereby lessening the uncertainties on the high energy behaviour of the positron fraction. Furthermore, the experiment is continuously taking data and the increased statistics will allow the measurement of the positron fraction to be extended up to an energy of about 300 GeV. The combination of these efforts will help in discriminating between various dark matter and pulsar models put forward to explain both our results and the ATIC[8] results. New important information will soon come also from the FERMI satellite that is studying the diffuse Galactic cosmic γ-ray spectrum. Pulsars are predominantly distributed along the Galactic plane, while dark matter is expected to be spherically distributed as an extended halo and highly concentrated at the Galactic Centre. The diffuse γ-ray spectrum is sensitive to these different geometries. Furthermore, PAMELA is measuring the energy spectra of both electrons (up to ~500 GeV) and positrons (up to ~300 GeV). These data will clarify if the ATIC results[8] are due to a significantly large component of pair-produced electrons and positrons (to explain the high energy ATIC data, the positron fraction should exceed 0.3 above 300 GeV), hence pointing to primary positron sources, or to a hardening of the electron spectrum with a more mundane explanation.

Received 28 October 2008; accepted 6 February 2009.

1. Moskalenko, I. V. & Strong, A. W. Production and propagation of cosmic-ray positrons and electrons. *Astrophys. J.* **493,** 694–707 (1998).
2. Atoian, A. M., Aharonian, F. A. & Volk, H. J. Electrons and positrons in the galactic cosmic rays. *Phys. Rev. D* **52,** 3265–3275 (1995).
3. Heinz, S. & Sunyaev, R. Cosmic rays from microquasars: A narrow component in the CR spectrum. *Astron. Astrophys.* **390,** 751–766 (2002).
4. Jungman, G., Kamionkowski, M. & Griest, K. Supersymmetric dark matter. *Phys. Rep.* **267,** 195–373 (1996).
5. Golden, R. L. *et al.* Measurement of the positron to electron ratio in the cosmic rays above 5 GeV. *Astrophys. J.* **457,** L103–L106 (1996).
6. Barwick, S. W. *et al.* Measurements of the cosmic-ray positron fraction from 1 to 50 GeV. *Astrophys. J.* **482,** L191–L194 (1997).
7. Aguilar, M. *et al.* Cosmic-ray positron fraction measurement from 1 to 30 GeV with AMS-01. *Phys. Lett. B* **646,** 145–154 (2007).
8. Chang, J. *et al.* An excess of cosmic ray electrons at energies of 300–800 GeV. *Nature* **456,** 362–365 (2008).
9. Picozza, P. *et al.* PAMELA — A payload for antimatter matter exploration and light-nuclei astrophysics. *Astropart. Phys.* **27,** 296–315 (2007).
10. Delahaye, T. *et al.* Galactic secondary positron flux at the Earth. Preprint at ⟨http://arXiv.org/abs/0809.5268v3⟩ (2008).
11. Boezio, M. *et al.* The cosmic-ray electron and positron spectra measured at 1 AU during solar minimum activity. *Astrophys. J.* **532,** 653–669 (2000).
12. Alcaraz, J. *et al.* Leptons in near earth orbit. *Phys. Lett. B* **484,** 10–22 (2000).
13. Clem, J. & Evenson, P. in *Proc. 30th Intl Cosmic Ray Conf.* Vol. 1 (eds Caballero, R. *et al.*) 477–480 (Universidad Nacional Autónoma de México, 2008).
14. Aharonian, F. *et al.* First detection of a VHE gamma-ray spectral maximum from a cosmic source: HESS discovery of the Vela X nebula. *Astron. Astrophys.* **448,** L43–L47 (2006).
15. Berezhko, E. G., Ksenofontov, L. T. & Völk, H. J. Emission of SN 1006 produced by accelerated cosmic rays. *Astron. Astrophys.* **395,** 943–953 (2002).
16. Serpico, P. On the possible causes of a rise with energy of the cosmic ray positron fraction. *Phys. Rev. D* **79,** 021302 (2009).
17. Komatsu, E. *et al.* Five-year Wilkinson microwave anisotropy probe observations: Cosmological interpretation. *Astrophys. J. Suppl. Ser.* **180,** 330–376 (2009).
18. Servant, G. & Tait, T. M. P. Is the lightest Kaluza-Klein particle a viable dark matter candidate? *Nucl. Phys. B* **650,** 391–419 (2003).
19. Cheng, H. C., Feng, J. L. & Matchev, K. T. Kaluza-Klein dark matter. *Phys. Rev. Lett.* **89,** 211301 (2002).
20. Bertone, G., Hooper, D. & Silk, J. Particle dark matter: Evidence, candidates and constraints. *Phys. Rep.* **405,** 279–390 (2005).
21. Adriani, O. *et al.* A new measurement of the antiproton-to-proton flux ratio up to 100 GeV in the cosmic radiation. *Phys. Rev. Lett.* **102,** 051101 (2009).
22. Cholis, I., Dobler, G., Finkbeiner, D. P., Goodenough, L. & Weiner, N. The case for a 700+ GeV WIMP: Cosmic ray spectra from ATIC and PAMELA. Preprint at ⟨http://arXiv.org/abs/0811.3641v1⟩ (2008).
23. Bergström, L., Bringmann, T. & Edsjö, J. New positron spectral features from supersymmetric dark matter: A way to explain the PAMELA data? *Phys. Rev. D* **78,** 103520 (2008).
24. Donato, F., Maurin, D., Brun, P., Delahaye, T. & Salati, P. Constraints on WIMP dark matter from the high energy PAMELA $\bar{p}/p$ data. *Phys. Rev. Lett.* **102,** 071301 (2009).
25. Grajek, P., Kane, G., Phalen, D. J., Pierce, A., &. and Watson, A. Is the PAMELA positron excess winos? Preprint at ⟨http://arXiv.org/abs/0812.4555v1⟩ (2008).
26. Grimani, C. Pulsar birthrate set by cosmic-ray positron observations. *Astron. Astrophys.* **418,** 649–653 (2004).
27. Büsching, I., de Jager, O. C., Potgieter, M. S. & Venter, C. A cosmic-ray positron anisotropy due to two middle-aged, nearby pulsars? *Astrophys. J.* **78,** L39–L42 (2008).
28. Yuksel, H., Kistler, M. D. & Stanev, T. TeV gamma rays from Geminga and the origin of the GeV positron excess. Preprint at ⟨http://arXiv.org/abs/0810.2784v2⟩ (2008).
29. Hooper, D., Blasi P. & Serpico, P. D. Pulsars as the sources of high energy cosmic ray positrons. *J. Cosmol. Astropart. Phys.* **01,** 025 (2009).
30. Beatty, J. J. *et al.* New measurement of the cosmic-ray positron fraction from 5 to 15GeV. *Phys. Rev. Lett.* **93,** 241102 (2004).

Supplementary Information is linked to the online version of the paper at www.nature.com/nature.

Acknowledgements We thank D. Marinucci for discussions concerning statistical methods, D. Müller, S. Swordy and their group at University of Chicago, G. Bellettini and G. Chiarelli for discussions about the data analysis and L. Bergström for comments on the interpretation of our results. We acknowledge support from The Italian Space Agency (ASI), Deutsches Zentrum für Luftund Raumfahrt (DLR), The Swedish National Space Board, The Swedish Research Council, The Russian Space Agency (Roscosmos) and The Russian Foundation for Basic Research.

Author Information Reprints and permissions information is available at www.nature.com/reprints. Correspondence and requests for materials should be addressed to P.P. (Piergiorgio.Picozza@roma2.infn.it).